Ecotoxicology and Environmental Safety 222 (2021) 112461

Contents lists available at ScienceDirect

Ecotoxicology and Environmental Safety

journal homepage: www.elsevier.com/locate/ecoenv

High-fat diet-induced aggravation of cardiovascular impairment in permethrin-treated Wistar rats

Anouar Feriani [a], Mariano Bizzarri [b], Meriam Tir [c], Nouf Aldawood [d], Hussah Alobaid [d], Mohamed Salah Allagui [e], Waleed Dahmash [d], Nizar Tlili [f], Kais Mnafgui [e], Saleh Alwasel [d], Abdel Halim Harrath [d,*]

[a] Research Unit of Macromolecular Biochemistry and Genetics, Faculty of Sciences of Gafsa, 2112 Gafsa, Tunisia
[b] Sapienza University of Rome, Dept of Experimental Medicine, Syst Biol Grp Lab, Rome, Italy
[c] Laboratoire des Sciences de l'Environnement, Biologie et Physiologie des Organismes Aquatiques, LR18ES41, Faculté des Sciences de Tunis, Université Tunis EL Manar, 2092 Tunis, Tunisia
[d] Department of Zoology, College of Science, King Saud University, P.O. Box 2455, Riyadh 11451, Saudi Arabia
[e] Laboratory of Animal Ecophysiology, Faculty of Science of Sfax, 3018 Sfax, Tunisia
[f] Institut Supérieur des Sciences et Technologies de l'Environnement, Université de Carthage, Tunisia

ARTICLE INFO

Edited by Professor Bing Yan

Keywords:
Permethrin
High-fat diet
Heart
Fibrosis
Oxidative stress

ABSTRACT

This study characterized the impact of post-weaning high-fat diet (HFD) and/or permethrin (PER) treatment on heart dysfunction and fibrosis, as well as atherogenic risk, in rats by investigating interactions between HFD and PER. Our results revealed that HFD and/or PER induced remarkable cardiotoxicity by promoting cardiac injury, biomarker leakage into the plasma and altering heart rate and electrocardiogram pattern, as well as plasma ion levels. HFD and/or PER increased plasma total cholesterol, triacylglycerols, and low-density lipoprotein (LDL) cholesterol levels but significantly reduced high-density lipoprotein (HDL) cholesterol. Cardiac content of per-oxidation malonaldehyde, protein carbonyls, and reactive oxygen species were remarkably elevated, while glutathione levels and superoxide dismutase, catalase and glutathione peroxidase activities were inhibited in animals receiving a HFD and/or PER. Furthermore, cardiac DNA fragmentation and upregulation of Bax and caspase-3 gene expression supported the ability of HFD and/or PER to induce apoptosis and inflammation in rat hearts. High cardiac TGF-β1 expression explained the profibrotic effects of PER either with the standard diet or HFD. Masson's Trichrome staining clearly demonstrated that HFD and PER could cause cardiac fibrosis. Additionally, increased oxidized LDL and the presence of several lipid droplets in arterial tissues highlighted the atherogenic effects of HFD and/or PER in rats. Such PER-induced cardiac and vascular dysfunctions were aggravated by and associated with a HFD, implying that obese individuals may be more vulnerable to PER exposure. Collectively, post-weaning exposure to HFD and/or PER may promote heart failure and fibrosis, demonstrating the pleiotropic effects of exposure to environmental factors early in life.

1. Introduction

Cardiovascular diseases (CVD) have risen dramatically over the past decades worldwide (Georgiadis et al., 2018). Some reports estimate that CVD mortality rates can reach up to 22.2 million individuals annually by 2030 (Ruan et al., 2019). Environmental pollutants, including the widespread use of pesticides, may explain the continuous increase in CVD (Georgiadis et al., 2018). New research has shown that direct occupational exposure to pesticides (Berg et al., 2019) and/or the consumption of food and water contaminated with these agrochemical pollutants (Chiu et al., 2019), contribute to the development of CVD. Several indices suggest that lipid profile disorders, inflammation, and oxidative stress linked to pesticide exposure may contribute to cardiovascular events (Feriani et al., 2020b). However, the exact mechanisms have not been fully elucidated.

Alternatively, recent epidemiological studies have implicated nutrition in the increasing prevalence of CVD. Reports have shown that dietary fats play an important role in cardiac dysfunction (Hamzeh et al.,

* Corresponding author.
E-mail address: hharrath@ksu.edu.sa (A.H. Harrath).

https://doi.org/10.1016/j.ecoenv.2021.112461
Received 31 December 2020; Received in revised form 12 June 2021; Accepted 23 June 2021

2017). At present, 49% of patients with heart disease have been characterized as overweight or obese (Csige et al., 2018). Experimental studies in rats fed a high-fat diet (HFD) have demonstrated that lipid accumulation can affect structural and functional changes in vascular and heart tissues (Ruan et al., 2019).

Some studies have reported that a HFD can aggravate lipophilic pesticide toxicity (Kondakala et al., 2017). As discussed earlier, obese animals are particularly susceptible to several pesticide intoxication, especially glucose metabolism dysfunction (Xiao et al., 2018), neuronal disturbances (Howell et al., 2018), respiratory injuries (El Khayat El Sabbouri et al., 2020), and obesogenic effect (Wang et al., 2017). However, limited research has been available concerning the prevalence of heart dysregulation.

Permethrin (PER), a type I synthetic pyrethroid, has been widely used in agricultural environments due to its excellent and efficient pest control capabilities (Saillenfait et al., 2018). Ingestion, inhalational, and dermal absorption have been considered the main pathways of PER exposure (Karmaus et al., 2016). PER is hazardous to animals and humans due to its widespread use and bioaccumulation in the environment. The dosage of PER used in this study (5 mg/kg) were established based on literature data for LD50 (500 mg/kg) (IRIS, 1998; WHO, 1996), and according to recent study reported by (Feriani et al., 2021). In the environment, typical reported concentrations are in the low ng/Kg range with the most contaminated areas showing values from 20 to 150 ng/kg in urban and agricultural runoffs (Hladik and Kuivila, 2009). The contents of PER in the food are as follows: lettuce 770–801 ng/kg, apple 194–510 ng/kg, spinach 54.9–48.6 μg/kg, and romaine lettuce 561–670 μg/kg (Li et al., 2016; Vonderheide et al., 2009). Although the PER amounts that people consume are lower than those used in our study, it has been reported that over time, PER can accumulate and cause damage. Animal exposed to PER have exhibited significant health disorders, including oxidative damage, hepatotoxicity, insulin intolerance, and neuronal disturbances (Fedeli et al., 2017; Jellali et al., 2018; Xiao et al., 2017). Although some studies have explored the effects of PER intoxication together with a normal-fat diet, no scientific report has investigated the impact of simultaneous exposure to both PER and HFD.

Considering that majority of individuals have diets closely resembling a HFD, our experimental design was tailored to investigate the impact of food risk factors, especially an unbalanced diet high in fat, and PER residues in order to draw attention toward the effects of extensively used environmental pollutants in a Western diet model.

In particular, the present work was designed to examine, for the first time in rats, the impact of subchronic post-weaning exposure to PER and/or HFD, focusing on cardiac function and related disorders. Thus, electrocardiogram (ECG) recordings, lipid profiles, and inflammatory, oxidative stress, and molecular markers were analyzed. Moreover, histological study of cardiac and aortic integrity verified using hematoxylin and eosin (H-E), Masson's trichrome, Oil Red O, and 2,3,5-triphenyltetrazolium chloride (TTC) staining] was conducted.

2. Materials and methods

2.1. Drugs and chemicals

PER (98% purity; Chemical Abstracts Service registry number: 52645-53-1) was purchased from Sigma-Aldrich (St. Louis, MO, USA). All other chemicals were purchased from either Sigma-Aldrich Co. (St. Louis, MO) or Fisher Scientific (Waltham, MA).

2.2. Animal preparation and induction of obesity using a high-fat diet

All experimental and animal (Wistar rats) welfare protocols were in accordance with ethical guidelines and were approved by the Tunisian Ethical Committee for the Care and Use of Laboratory Animals. All experiments were conductedon40 one-month-old male rats after weaning. Rats were subsequently divided into two groups: Group 1 (n = 20; negative control receiving standard diet for 2 months) and Group 2 (n = 20; positive control receiving a HFD containing 10% of butter and 1% of cholesterol for 2 months to induce obesity)(Dziadek et al., 2019). The composition of obesity diets is shown in Table 1.

At 3 months of age, blood was withdrawn through retro-orbital puncture to verify obesity status. Plasma lipid biomarker [total cholesterol (TC), triacylglycerols (TG), high-density lipoprotein cholesterol (HDL-C), and low-density lipoprotein cholesterol (LDL-C)] concentrations were then determined.

2.3. Experimental design

After confirming hyperlipidemic status, animals were divided into four groups (n = 10) and received the following treatment schedule:(1) Control group comprising control animals receiving standard diet and vehicle (corn oil) for 12 weeks successively;(2) HFD group comprising obese animals receiving a HFD and vehicle (corn oil) for 12 weeks successively;(3) PER group comprising normal animals receiving standard diet and a gavage-administered PER suspension in corn oil at a dose of 5 mg/kg b.w. (1/100 LD_{50})daily for 12 weeks successively; and (4) HFD + PER group comprising obese animals receiving a HFD and a gavage-administered PER suspension in corn oil at a dose of 5 mg/kg b.w. daily for 12 weeks successively.

Insecticide doses were selected based on literature data for LD50 (500 mg/kg) and considering the "no observed adverse effect level," which is 5 mg/kg for PER (IRIS, 1998; WHO, 1996). The conduct of the study for 12 weeks is based on our recent research (Feriani et al., 2021), in which have shown that a subchronic exposure by permethrin induces toxicity in rats. Animals were housed in plastic cages with a 12 h/12 h dark/light cycle in a temperature- and humidity-controlled room. Rats were fed diets and water adlibitum. Fasting feed intake and body weight were measured periodically every week.

2.4. Electrocardiography

For electrocardiography, rodents were anaesthetized and placed in the supine position on a board, after which needle electrodes were attached to the skin of all animals at position II. Thereafter, electrocardiography was performed using an electrocardiograph (ECG VET 110, Biocare, China), with the obtained recordings being photographed.

2.5. Biological sample collection

After electrocardiography, the animals were anesthetized with a solution of ketamine hydrochloride (30 mg/kg b.w.) and then sacrificed. Blood samples were collected and centrifuged (3500 rpm, 10 min, 4 °C) to obtain plasma and then stored at −20 °C for biochemical marker estimation. Cardiac and aortic tissues were removed, washed with phosphate buffer saline, and weighed. Organ fragments were snap-frozen in liquid nitrogen and then stored at −80 °C for further

Table 1
The composition of HFD diets.

Ingredient	Amount (g/kg)
Corn starch	480.5
Sucrose	95
Casein	205
Soybean oil	0
Butter	105
Cholesterol	11
Fiber	50
Mineral mix	40
Vitamin mix	10
Choline	4.1
Tert-Butylhydroquinone	0.01

molecular and biochemical analyses. Another batch of fresh cardiac and aortic fragments were immediately used for TTC and Oil Red O analysis, respectively. The remaining tissues were directly preserved in a neutralized formalin (10%) solution for histopathological examinations using the paraffin technique.

2.6. Lipid concentration measurement

Plasma TG, TC, HDL-C, and LDL-C levels were determined using a blood analyzer with commercial kits (Biomaghreb, Tunisia) as per the manufacturer's instructions. Oxidized LDL levels were measured in the LDL fraction using enzyme-linked immunosorbent assay (ELISA) kits according to the manufacturer's instructions (USCN Life Science Inc., Wuhan) and were presented in ng/μg LDL protein. Various parameters related to atherosclerosis were determined using the following formula: Cardiac risk ratio (CRR) = (TC/HDL-C) and Atherogenic coefficient (AC) = (TC-HDL-C/HDL-C).

2.7. Cardiac biomarker estimation

Aspartate aminotransferase (AST), lactate dehydrogenase (LDH), and creatine kinase-MB (CK-MB) activities in the plasma were determined using various commercially available kits (Biomaghreb, Tunisia) following the manufacturer's instructions. Content of plasma concentrations of Na^+, K^+, Cl^-, and Ca^{2+} were determined using an ionogram analyzer (EasyLyte Plus, Medica, France). Plasma cardiac troponin (cTn-I) and C-reactive protein (CRP) levels were determined using a Rat ELISA assay kit (Boster, Wuhan, China) following the manufacturer's instructions.

2.8. Analysis of tumor necrosis factor alpha and interleukin-6 in plasma and heart homogenates

Plasma and cardiac tissue levels of tumor necrosis factor alpha (TNF-α) and interleukin-6 (IL-6) were determined using ELISA (QUIAGEN Company, USA) following the manufacturer's instructions (Vector Laboratories, NJ, USA), and expressed as μg/mL and μg/mg tissue, respectively.

2.9. Analysis of oxidative stress markers

Catalase (CAT)(Aebi, 1984), superoxide dismutase (SOD)(Marklund and Marklund, 1974), and glutathione peroxidase (GPx)(Flohe and Gunzler, 1984)activities, as well as reduced glutathione (GSH) (Ellman, 1959), peroxidation malonaldehyde (MDA)(Buege and Aust, 1978),and protein carbonyl (PC) (Levine et al., 1990)concentrations, in heart tissues were determined via the spectrophotometric method using various commercially available kits (Nanjing, China) following the manufacturer's instructions. Reactive oxygen species (ROS) levels (% of controls) were calculated using the spectrofluorimetric method, as previously described by (Gargouri et al., 2018). Protein levels of cardiac homogenate were measured to estimate activity per mg protein.

2.10. Apoptosis assessment through DNA fragmentation

A semi-quantitative method was utilized to detect apoptosis via electrophoresis. Cardiac tissue genomic DNA in control and treated rats were isolated using the phenol-chloroform DNA extraction method. The separation of intact and fragmented DNA fractions was visualized in an agarose gel using ethidium bromide staining, following the protocol of described by (Feriani et al., 2020b).

2.11. Gene expression analysis

Reverse transcriptase polymerase chain reaction (RT-PCR) analysis was conducted to explore the differential expression of various genes involved in apoptosis and fibrosis of cardiac tissue. Total cardiac tissue RNA was isolated using TRIzol reagent (Invitrogen, Carlsbad, USA) as per the manufacturer's instructions. Reverse transcription was performed with 2 μg of extracted mRNA using superscript reverse transcriptase (Invitrogen, France). Amplification was achieved using gene specific primers as shown in Table 2. Real-time cycler conditions were determined as described by (Feriani et al., 2020b). Amplicons were electrophoresed on 1.2% agarose gel and visualized through ethidium bromide staining. Amplicon band intensity was analyzed using Image J software withβ-actin as a control.

2.12. Estimation of cardiac damage using 2,3,5-triphenyltetrazolium chloride staining

Cardiac injury, such as local infarction, was explored using the protocol reported by Feriani et al. (2020a). Briefly, freshly isolated cardiac tissues from all experimental rats were immerged in a solution containing TTC at room temperature (37 °C) for 15 min. Accordingly, normal tissues appeared red, while altered areas turned white.

2.13. Analysis of histological structure and fibrosis status

Heart tissues were fixed in 10% formalin solution for 7 days and then introduced into paraffin liquid. The obtained blocks were cut into 5 μm sections and stained with H-E to evaluated changes in cardiac structure. Masson's Trichrome staining was employed to determined cardiac collagen deposition, as described previously by (Feriani et al., 2020b). Histological sections were analyzed via a light microscopic and then photographed. Thereafter, histopathological cardiac alterations were scored as follows using the semi-quantitative percentage of damaged area: 0, none; 0.5, < 10%; 1, 10–25%; 2, 25–50%; 3, 50–70%; and 4, > 75% (Kim et al., 2016). Image analysis for the quantification of collagen deposition in six randomly selected microscopic fields per specimen was performed using Image J.

2.14. Immunohistochemical detection

TGF-β1 expression was determined using immunohistochemistry. Accordingly, 5 μm slides were incubated in the dark with H_2O_2 (3%) for 15 min at 37 °C and then washed thrice with phosphate-buffered saline. Thereafter, samples were incubated with primary antibodies at 4 °C overnight. After three cycles of phosphate-buffered saline washing, secondary antibodies were added onto the slides, which were then incubated at 37 °C for 30 min. The sections were incubated with horseradish peroxidase-labeled avidin at 37 °C for 30 min. DAB was added onto the slides and left to react until the reaction was stopped by ddH_2O. Finally, the samples were re-stained using hematoxylin, after which immunohistochemical sections were analyzed using a light microscopic and then photographed at 200 × magnification.

2.15. Oil red O staining

Aortic tissues were removed, fixed in formaldehyde (4%), and analyzed using the "en face" method as reported by (Kim et al., 2013).

Table 2
Primers used in RT-PCR study.

Gene	Primers
NF-ƙB	Sense primer: GCCGTGGAGTACGACAACATC Antisense primer: TTTGAGAAGAGCTGCCAGCC
Caspase-3	Sense primer: CAGAGCTGGACTGCG GTATTGA Antisense primer: AGCATGGCGCAA AGTGACTG
Bax	Sense primer: TTCATCCAGGAT CGAGCAGA Antisense primer: GCA AAGTAG AAGGCA ACG
β-actin	Sense primer: GGAGATTACTGCCCTGGCTCCTA Antisense primer: GACTCATCGTACTCCTGCTTGCTG

Briefly, tissues were opened longitudinally and placed in isopropanol solution for 3 min, followed by 60 min of Oil Red O staining to identify atherosclerotic lesions. The obtained section was photographed and analysis. The red stained surface indicated atherosclerotic lesions, which was evaluated (%) using NIH Image J software.

2.16. Statistical analysis

Statistical analyses comprising of one-way analysis of variance and Tukey's test were performed using GraphPad Prism 4.02 for Windows, with $p < 0.05$ indicating statistical significance.

3. Results

3.1. Body weight and food intake

As shown in Table 3, animals fed a HFD and/or PER had significantly greater weight gain ($P < 0.05$) compared to those fed a standard diet (control). Although the relative heart weight remained unchanged in the HFD group, cardiac hypertrophy was observed in PER-treated animals, with the HFD+PER group exhibiting significantly greater hypertrophy compared to the PER group ($P < 0.05$). This result was confirmed during morphologic study of heart tissues (Fig. 1A).

3.2. Electrocardiogram findings and heart rate

Data shown in Fig. 1B and C revealed that normal animals exhibited normal ECG patterns with regular sinus rhythm and heart rate (195 ± 11.21 bpm). Compared to animals fed a standard or HFD, normal or HFD rats exposed to PER (5 mg/kg b.w.) exhibited significantly greater disruption in electrocardiographic pattern, including decreased Ramplitude, ST segment elevation (Fig. 1D), and a marked increase in heart rate (310 ± 8 bpm) with auricular flutter, indicating the onset of a myocardial infarction event. This dysregulation in ECG pattern was aggravated in the HFD+PER group, with a heart rate of 385 ± 4 bpm.

3.3. Lipid profile and atherogenic parameters

Several lipid biomarkers were calculated (Table 4). Compared to the control group, the HFD or PER group exhibited significantly higher elevation ($P < 0.05$) in plasma TC, TG, and LDL-C and decrease ($P < 0.05$) in HDL-C, with the HFD + PER group exhibiting a significantly worse lipid profile compared to the treatment groups ($P < 0.05$). Similarly, all treatment groups showed significantly higher levels ($P < 0.05$) of markers predicting atherosclerosis risk (AC and CRR) compared to the control group.

3.4. Cardiac injury marker enzymes

As shown in Table 5, the HFD group exhibited significantly higher ($P < 0.05$) AST, CK-MB, and LDH activities, without affecting CRP and cTn-T levels, compared to the control group. Furthermore, normal or HFD rats exposed to PER (5 mg/kg b.w.) exhibited significantly clearly greater ($P < 0.05$) AST, CK-MB, LDH activities, as well as CRP and cTn-T levels, compared to the control or HFD group. The HFD + PER group had even worse values for the aforementioned parameters compared to the other treatment groups.

Table 3
Gain and Heart weight index in control and experimental rats.

	Control	HFD	PER	HFD+PER
Gain weight (g)	100.6 ± 2.94	150.3 ± 2.47*	138.9 ± 1.71*	175.4 ± 2.02*¥
Heart weight index	0.34 ± 0.01	0.35 ± 0.03	0.39 ± 0.04*	0.44 ± 0.02*¥

Values are expressed as mean ± SD of ten rats in each group.
* $P < 0.05$ significant differences compared to controls.
¥ $P < 0.05$ significant differences compared to HFD or PER group of rats.
HFD: High Fat Diet
PER: Permethrin

3.5. Plasma electrolytes

Plasma electrolyte levels in all treated animals are summarized in Table 6. Our results showed no significant changes in plasma K^+, Na^+, Cl^-, and Ca^{2+}levels between normal and obese animals. However, the PER group exhibited significantly higher ($P < 0.05$) plasma K^+ and Ca^{2+} levels and significantly lower ($P < 0.05$) Na^+ and Cl^-levels compared to the control or HFD group.

3.6. Tumor necrosis factor alpha and interleukin-6 levels

Pro-inflammatory cytokine levels in the plasma and heart of treated rats are shown in Fig. 1E and F. Compared to the control group, the HFD group had significantly higher ($P < 0.05$) plasma and cardiac TNF-α and IL-6 levels. Conversely, the PER group exhibited significantly higher TNF-α and IL-6 levels ($P < 0.05$) compared to the HFD group, suggesting inflammation in plasma and cardiac tissue. Both pro-inflammatory markers were amplified in the HFD+PER group.

3.7. Cardiac oxidative profile

Table 7 presents the levels and activities of oxidative stress biomarkers in the cardiac tissue of the treatment groups. Accordingly, MDA, PC, and ROS levels were significantly higher in the HFD+PER ($P < 0.05$) than in the HFD, PER, and control groups. Furthermore, obese rates exposed to PER had significantly lower CAT, SOD, and GPx activities, as well as GSH content ($P < 0.05$) relative to the all other animals. A significant difference in cardiac oxidative profile was observed between the normal group and HFD or PER group.

3.8. DNA ladder fragmentation

Results for DNA fragmentation analyses through agarose gel electrophoresis in all experimental animals are shown in Fig. 2. The genomic DNA extracted from the heart in the control (lane 2) or HFD (lane 3) group revealed an intact band. However, DNA laddering, a key feature of apoptosis, was observed in hearts of PER-treated animals receiving either a standard diet (lane 4) or HFD (lane 5). Our results revealed that the HFD + PER group exhibited more harmful cardiac DNA damage than the PER group.

3.9. Gene expression using reverse transcriptase polymerase chain reaction

The expression of NF-κB, Bax, and Caspase 3 in the myocardial tissues of normal and experimental rats by RT-PCR are shown in Fig. 2B. Densitometric analysis of these markers is shown in Fig. 2C. The HFD group exhibited significantly higher NF-κB mRNA expression compared to the control group, with Caspase 3 and Bax in heart tissue being unaffected. However, PER administration upregulated the expression of the aforementioned parameters. The impact of a HFD on these cardiac genes was further increased following PER exposure given their remarkably higher levels in the HFD + PER group compared to the HFD or PER group.

3.10. Analysis of heart injury via 2,3,5-triphenyltetrazolium chloride staining

TTC staining results in all treatment animals are shown in Fig. 3A. Analysis of cardiac sections from the control or HFD group showed a red

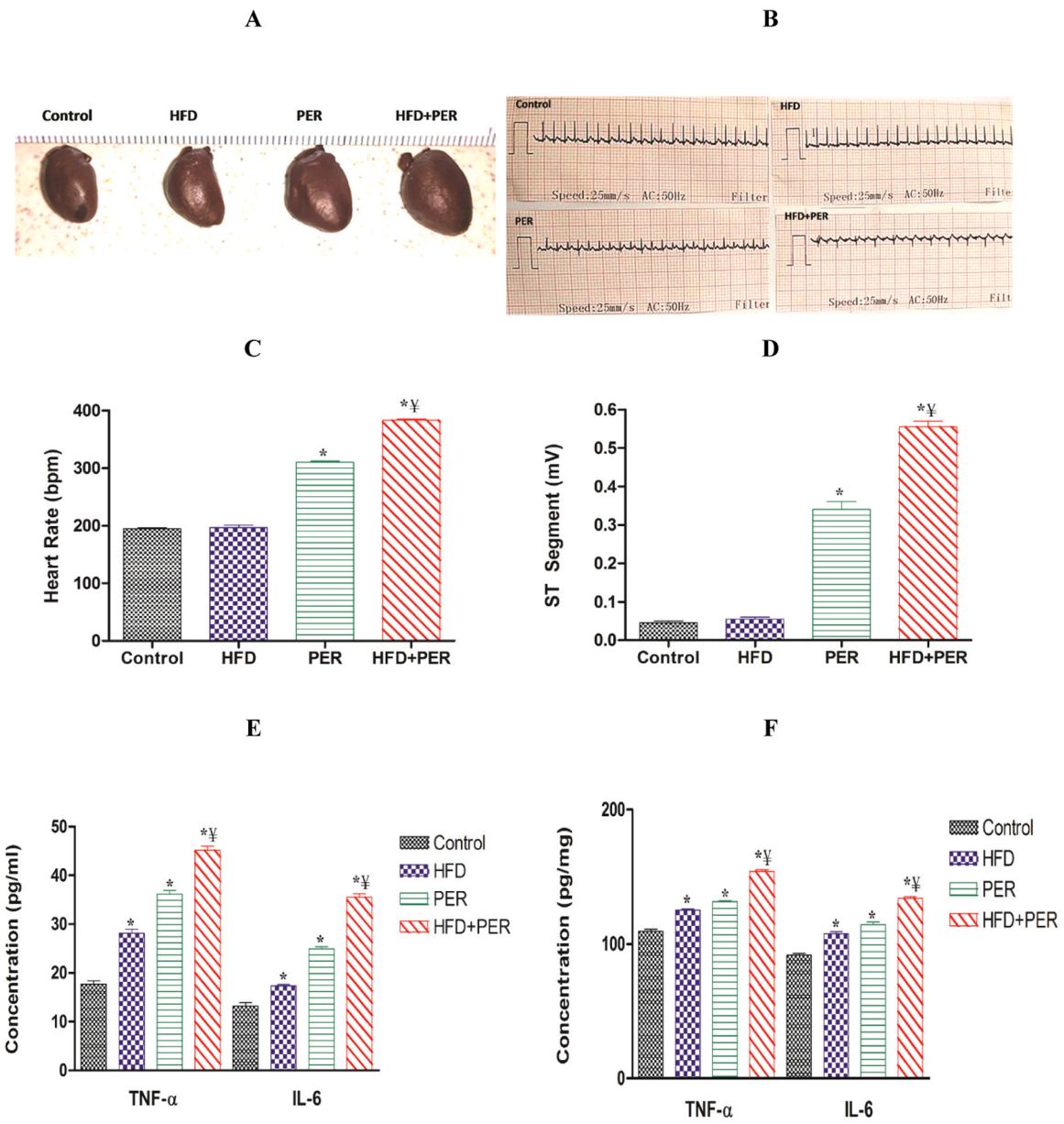

Fig. 1. Impact of a high-fat diet (HFD) and/or permethrin (PER) treatment on heart morphology (A), electrocardiogram (ECG) patterns (B), heart rate(C), and ST-segment(D)in control and experimental animals. Control and HFD groups exhibited a normal heart structure and ECG pattern. The PER group exhibited hypertrophy and pathological changes, such as decreased R-amplitude, ST-segment elevation, and marked increase in heart rate. The HFD + PER group showed aggravation in ECG patterns. bpm: beats per minute. (E-F) Effect of a high-fat diet (HFD) and/or permethrin (PER) on the concentration of proinflammatory cytokines (tumor necrosis factor alpha and interleukin-6) in either plasma (E) or heart tissues (F) analyzed using sandwich enzyme-linked immunosorbent assay. Values are expressed as mean ± standard deviation for the 10 rats in each group. * $P < 0.05$ significant differences compared to controls. ¥ $P<0.05$ significant differences compared to the HFD or PER group.

color, indicating a normal structure. Interestingly, PER administration in either the control or HFD-treated animals revealed a pale white color, indicating a state of necrosis in the heart tissue. Infarct or ischemic size quantification showed that the HFD+PER exhibited greater heart tissue injury compared to all other groups (Fig. 3B).

3.11. Histology analysis

Histological analysis results of the heart structure via H-E staining in all experimental animals is presented in Fig. 4. Compared to the normal group, obese or PER-exposed rats exhibited more injuries, including cardiomyocyte vacuolization, inflammatory cell infiltration, and myocardial tissue separation. Furthermore, subchronic PER exposure in obese rats amplified the harmful effects on cardiac tissue.

3.12. Collagen deposition and myocardial fibrosis

Masson's Trichrome was used to examine myocardial fibrosis. Microscopic observation (Fig. 5) revealed that the HFD or PER group had greater collagen accumulation in heart tissue increased in compared to the control group, with the HFD + PER group having even great collagen deposition. In fact, a state of cardiac fibrosis had been established following the appearance of intense fibrous collagen bridges in cardiac tissue, which is manifested by the higher blue color intensity in all treatment groups compared to the normal group.

3.13. Immunohistochemical detection

TGF-β1 distribution determined using immunochemical assays is

Table 4
Plasmatic lipid profile parameters and markers predicting the risk of atherosclerosis and cardiovascular disease in control and experimental rats.

	Control	HFD	PER	HFD+PER
TC (mg/dL)	47.33 ± 2.85	65.10 ± 3.25*	59.32 ± 2.69*	79.82 ± 2.79 *¥
TG (mg/dL)	38.33 ± 1.93	51.97 ± 2.32*	49.11 ± 1.68*	62.75 ± 2.24 *¥
LDL-C (mg/dL)	30.83 ± 2.01	43.91 ± 1.91*	40.1 ± 1.71*	61.43 ± 2.24 *¥
HDL-C (mg/dL)	41.32 ± 2.46	28.68 ± 1.8*	33.15 ± 1.32*	24.28 ± 1.81 *¥
Atherogenic coefficient (AC)	0.14 ± 0.05	1.27 ± 0.12	0.79 ± 0.14*	2.3 ± 0.27 *¥
Cardiac risk ratio (CRR)	0.87 ± 0.03	2.27 ± 0.12	1.79 ± 0.14*	3.3 ± 0.27 *¥

Values are expressed as mean ± SD of ten rats in each group.
*$P <$ 0.05 significant differences compared to controls.
¥ $P<0.05$ significant differences compared to HFD or PER group of rats.
HFD: High Fat Diet
PER: Permethrin

Table 5
Variation in the activities of creatine kinase-MB (CK-MB), lactate dehydrogenase (LDH), aspartate aminotransferase (AST), and cardiac troponin I (cTn-I) and C reactive protein (CRP) levels in plasma of control and experimental groups of rats.

Parameters	Control	HFD	PER	HFD+PER
CK-MB (U/L)	153.2 ± 3.51	172.0 ± 3.2*	182.5 ± 3.59*	192.9 ± 2.4*¥
LDH (U/L)	131.7 ± 2.35	139.9 ± 1.63*	153.0 ± 1.38*	163.9 ± 1.41*¥
AST (U/L)	108.9 ± 2.38	142.5 ± 2.79*	153.1 ± 1.76*	173.6 ± 3.66*¥
cTn-I (ng/mL)	0.21 ± 0.02	0.23 ± 0.03	1.42 ± 0.06*	1.89 ± 0.08*¥
CRP (pg/mL)	38.92 ± 3.18	38.02 ± 2.85	55.99 ± 3.11*	71.71 ± 3.84*¥

Values are expressed as mean ± SD of ten rats in each group.
*$P <$ 0.05 significant differences compared to controls.
¥ $P<0.05$ significant differences compared to HFD or PER group of rats.
HFD: High Fat Diet
PER: Permethrin

Table 6
Variation in plasma levels of Na^+, K^+, Cl^- and Ca^{2+} in control and experimental groups of rats.

Parameters	Control	HFD	PER	HFD+PER
Na^+ (mmol/L)	100.4 ± 3.56	100.9 ± 5.16	82.53 ± 4.23*	74.86 ± 1.04*¥
K^+ (mmol/L)	6.88 ± 0.62	6.77 ± 0.54	11.15 ± 1.01*	16.08 ± 1.81*¥
Cl^- (mmol/L)	84.01 ± 2.19	82.86 ± 2.26	71.72 ± 2.26*	67.77 ± 3.68*¥
Ca^{2+} (mmol/L)	13.19 ± 1.88	13.51 ± 1.99	21.98 ± 1.66*	27.61 ± 1.1*¥

Values are expressed as mean ± SD of ten rats in each group.
*$P <$ 0.05 significant differences compared to controls.
¥ $P<0.05$ significant differences compared to HFD or PER group of rats.
HFD: High Fat Diet
PER: Permethrin

shown in Fig. 6. The HFD and PER groups exhibited significantly greater TGF-β1 expression in heart tissue compared to the control group. Moreover, HFD rats exposed to PER had higher TGF-β1 levels compared to the HFD or PER group.

3.14. Oxidized low-density lipoprotein levels

Fig. 7 A presents the oxidized LDL levels in the plasma and aortic tissues of the treatment groups. The HFD + PER group had significantly higher plasma and aortic tissue oxLDL levels ($P < 0.05$) than the HFD, PER, and control groups. A significant difference in the oxidized LDL profile was observed between the HFD or PER group and the normal group.

Table 7
The change in TBARS, protein carbonyl (PC), ROS (reactive oxygen species), and endogenous antioxidants contents (GSH, SOD, CAT and GPX) in cardiac tissue in control and experimental rats.

Parameters	Control	HFD	PER	HFD+PER
TBARS (nmoles MDA/g tissue)	3.64 ± 0.52	8.69 ± 0.65*	8.98 ± 0.27*	15.32 ± 2.37*¥
PC (nmoles/mg protein)	1.11 ± 0.15	1.61 ± 0.15*	1.76 ± 0.11*	2.45 ± 0.27*¥
ROS (%)	44.87 ± 3.04	61.81 ± 2.82*	59.71 ± 3.04*	79.1 ± 0.01*¥
GSH (U/mg protein)	15.69 ± 1.33	11.56 ± 1.34*	12.09 ± 2.09*	6.99 ± 0.53*¥
CAT (U/mg protein)	19.43 ± 1.19	15.24 ± 1.1*	13.75 ± 1.41*	9.23 ± 1.04*¥
SOD (U/mg protein)	13.51 ± 1.82	8.98 ± 0.44*	8.89 ± 0.36*	5.41 ± 0.49*¥
GPx U/mg protein)	8.26 ± 0.49	5.86 ± 0.63*	4.75 ± 0.45*	2.8 ± 0.51*¥

Values are expressed as mean ± SD of ten rats in each group.
*$P <$ 0.05 significant differences compared to controls.
¥ $P<0.05$ significant differences compared to HFD or PER group of rats.
HFD: High Fat Diet
PER: Permethrin
h-fat diet or permethrin group.

3.15. Lipid deposition via Oil Red-O staining

To evaluate lipid deposition, frozen aortic sections from the control and treatment animals were examined using Oil Red O staining. As shown in Fig. 7B, normal structures without lipid droplets were observed in aortic tissues of control rats. However, arterial tissues of obese rate or those exposed to PER showed an increased lipid deposits (red color) in the thickened intima. The HFD+ PER group showed a significantly greater increase in lipid droplets compared to the HFD or PER group.

4. Discussion

While pesticide exposure or HFD consumption have been link to heart dysfunction among humans and animals (Feriani et al., 2020d; Ruan et al., 2019), little information currently exists regarding the synergistic actions of environmental pesticide exposure and a HFD on the cardiovascular system. As such, the current study aimed to characterize the effects of post-weaning PER exposure in the absence or presence of HFD, investigating cardiac structure/function and related disturbances. Data obtained herein revealed that subchronic PER exposure (3 months) significantly increased weight gain in either normal or HFD rats. This finding could be attributed to the neurotoxic effects of PER that accumulate in the nervous system, resulting in reduced

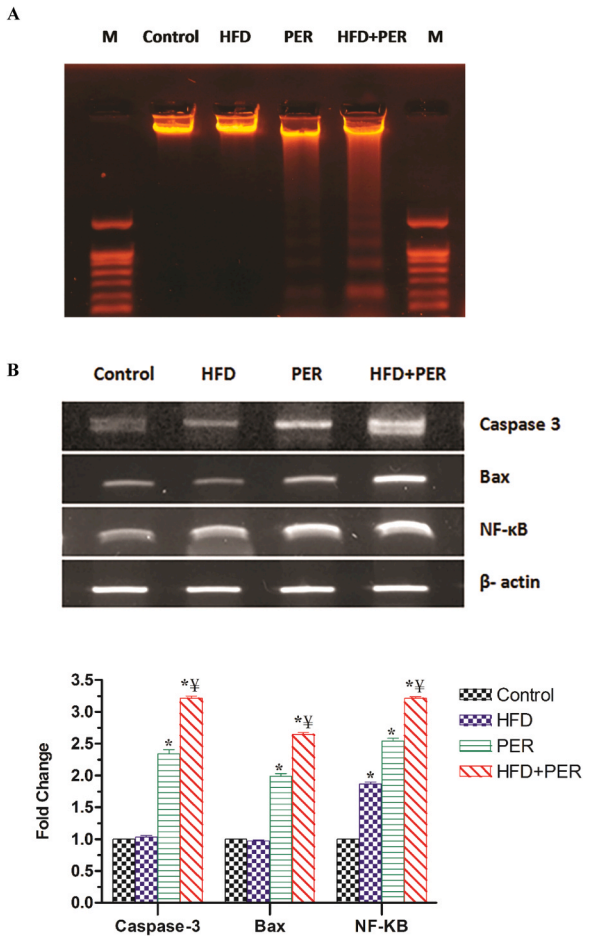

Fig. 2. Agarose gel electrophoretic pattern of DNA (A) and reverse transcriptase polymerase chain reaction analysis of NF-κB, Caspase 3, and Bax expression (B) and quantification of these genes (C) in cardiac tissues of control and experimental rats. M: size markers. Values are expressed as mean ± standard deviation for the 10 rats in each group. *$P<0.05$ significant differences compared to controls. ¥ $P<0.05$ significant differences compared to the HFD or PER group.

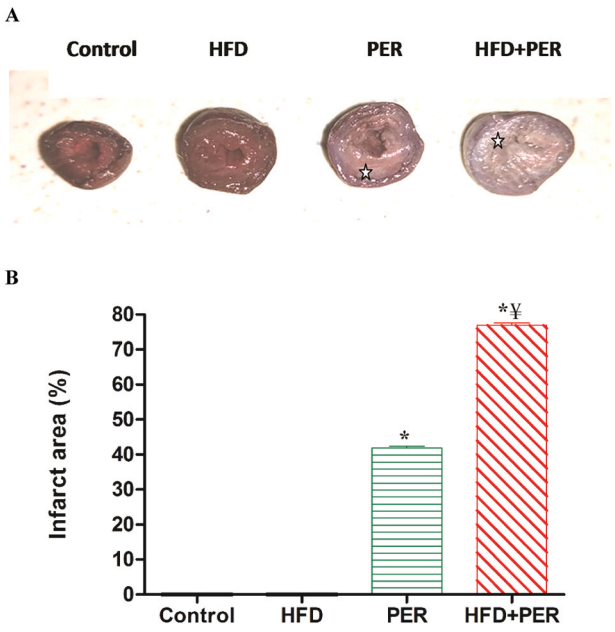

Fig. 3. Impact of a high-fat diet (HFD) and/or permethrin (PER) treatment on myocardial tissues in control and experimental rats using TTC staining (A) and myocardial infarct size quantification (%) (B). Values are expressed as mean ± standard deviation for the 10 rats in each group.* $P<$ 0.05 significant differences compared to controls. ¥ $P<0.05$ significant differences compared to the HFD or PER group.

voluntary activities and decreased energy expenditure (Xiao et al., 2017). Conversely, a study reported by (Howell et al., 2015) found that there were no significant differences in body weight between animals treated with persistent organic pollutants (2.0 mg/kg) in the HFD groups compared to the control group. Furthermore, although the relative heart weights of rats in the HFD or PER group were unaffected, a cardiac hypertrophy had been observed in the HFD + PER group resulting from leucocyte infiltration related to fibrosis (Prasad et al., 2017). In addition, Xiao et al. (2018) showed results contradictory to those found here, which mentioned a decrease in the weight of cardiac tissue in HFD groups treated with permethrin at doses of 500 and 5000 μg / kg.

The current study observed abnormalities in the ECG pattern, including ST elevation, unidentifiable P wave, and tachycardia, in the PER group, with the HFD+PER group exhibiting worse abnormalities. This suggested that HFD might aggravate PER-induced alterations in cardiac structure/function. Similar findings have been reported by (Patel et al., 2015) who showed that HFD-treated rats exhibited significantly worse cardiac electrical conduction disturbances in the presence of bisphenol.

The observed disturbance in physiological parameters had been confirmed by the elevated plasma LDH, ALT, AST, and CK-MB activities, as well as increased troponin-T levels, after PER exposure either in normal or HFD rats. The release of such markers indicates impaired membrane permeability and cell death in various tissues of the body including the heart, as previously reported (Feriani et al., 2020b), with such finding being consistent with histopathological analyses. H-E staining of heart tissue from the PER and HFD+PER groups revealed notable injuries, particularly cytoplasmic vacuolation, necrosis, interstitial edema, and excessive leukocyte infiltration. Recent studies corroborating such findings have demonstrated that deltamethrin, a synthetic pyrethroid, could induce cardiac tissue damage in laboratory animals (Feriani et al., 2020d).

Interestingly, the current results suggested that a HFD aggravated cardiac damage in PER-exposed rats. Indeed, substantial evidence has reported that PER is better absorbed and bioaccumulated in a HFD compared to a standard diet given its lipophilic characteristics (Xiao et al., 2018). Data from published studies have reported on the implications of lipid parameter disruption in the development of ischemic heart disease (Vijayakumar and Nachiappan, 2017). The current study found a considerable elevation in plasma TC, TG, and LDL-C and a remarkable decreased in HDL-C in all groups, with HFD rats exposed to PER exhibiting greater changes. Conversely, permethrin treatment at dose of 50 and 500 μg/kg significantly increased blood insulin, but no effect was observed on triglycerides, cholesterol, high fat-density lipoprotein, and low-density lipoprotein cholesterol levels in HFD animals (Xiao et al., 2017). Several mechanisms can explain the increase in such lipid biomarkers following pyrethroid exposure, some of which are linked to an excessive hepatic lipid synthesis (Feriani et al., 2020a) and/or to the suppression of certain receptors responsible for the clearance of lipid and lipoproteins (Feriani et al., 2020c).

A HFD has been known to significantly increase fat synthesis and accumulation in an organism (Liu et al., 2016). Thus, a HFD might increase the internalization of PER, a lipophilic molecule, in adipose-rich tissues, which could disturb lipid metabolism and promote subsequent abnormalities.

Several studies have supported the important role of oxidative stress in the pathophysiology of heart failure (Salmas et al., 2017; Talas et al., 2014; van der Pol et al., 2019). Our results clearly revealed that HFD and/or PER increased the content of cardiac oxidative stress markers

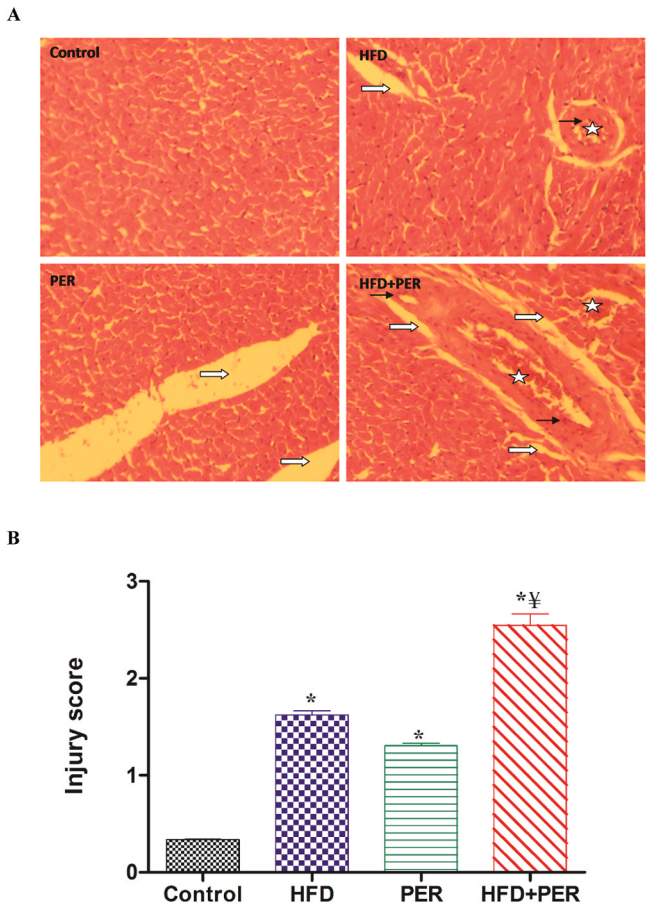

Fig. 4. Photomicrographs of cardiac tissues in all treatment animals. Heart tissue samples stained with hematoxylin and eosin (H-E; G × 200) (A) and scored using the semi-quantitative percentage of damaged area (B). Histological analysis showed hemorrhage (), inflammatory cell infiltration (), and myocardial tissue separation (). Values are expressed as mean ± standard deviation for the 10 rats in each group. *$P<0.05$ significant differences compared to controls. ¥ $P<0.05$ significant differences compared to HFD or PER group of rats.

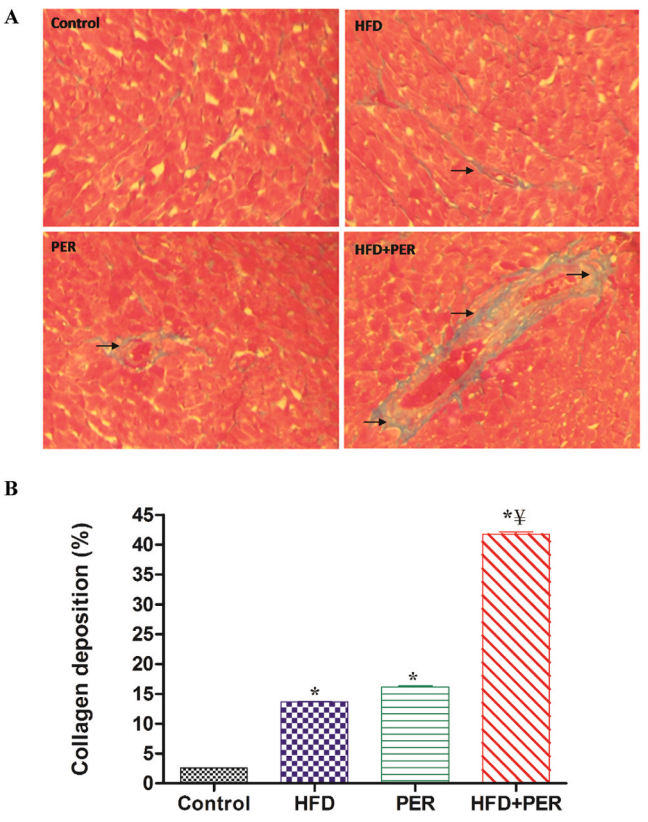

Fig. 5. : Photomicrographs of myocardial tissues in control and experimental treated rats (G × 200). Heart tissue sections stained with Masson's trichrome (MT) (A) and scored by quantifying collagen deposition and myocardial fibrosis (B). Collagen was identified in the cardiac tissue for high-fat diet (HFD), permethrin (PER), and HFD + PER groups and indicated by a blue color (black arrow). Values are expressed as mean ± standard deviation for the 10 rats in each group. *$P<0.05$ significant differences compared to controls. ¥ $P<0.05$ significant differences compared to HFD or PER group of rats.

(MDA and PC) and inhibited the activity of endogenous antioxidants (GSH, SOD, CAT, and GPx). Accordingly, (Csige et al., 2018) and (Feriani et al., 2020d) had suggested oxidative stress as a potential mechanism for obesity- or pyrethroid-induced cardiotoxicity. Contradicting this study, HFD induces cardiac oxidative stress without modifying cardiac antioxidant defense and lipid content in obese pigs (Li et al., 2017).

Advancements in cardiovascular research have suggested that oxidative stress-related apoptosis was an important pathway in the development of ischemic lesion and participated in the process of subsequent cardiac remodeling (Sousa et al., 2019). Our findings showed that the PER and HFD + PER groups had greater Bax and caspase 3 expression, both proapoptotic genes, compared to the controlor HFD group. This finding could suggest the activation of apoptotic pathways and stimulation of cardiac cell dysfunction and damage.

Recent reports corroborating these results have demonstrated that several synthetic pyrethroids could induce elevated expression of apoptotic genes in various animal tissues (Feriani et al., 2020c; Kumar et al., 2015).

Interestingly, the appearance of clear cardiac DNA fragments in animals receiving doses of PER with a standard or HFD supports the observed apoptosis event. These results were consistent with those suggested by Feriani et al. (2020) who indicated that pyrethroid administration induced DNA fragmentation in heart tissues via free radical generation. Findings obtained herein suggested that a HFD facilitates PER diffusion into the cell membrane and could mediates free radical production, which stimulates upregulation of Bax and caspase 3 mRNA and induces cardiac cell dysfunction, apoptosis, and genotoxicity. This effect could partly explain the observed amplification of oxidative stress, DNA fragmentation, and apoptosis in the HFD+PER group. Findings from multiple studies have suggested that a HFD increases susceptibility to pesticide-induced apoptosis in several tissues (Nan et al., 2020; Zhang et al., 2020).

Additionally, the current study demonstrated that normal or obese animals receiving PER exhibited elevated plasma Ca^{2+} levels, with the HFD + PER group exhibiting significantly greater levels. Given that calcium released from the cell must re-enter the cell for continuous cardiac contraction and relaxation, uncontrolled calcium cycling could induce abnormal cardiac function (Cui et al., 2018). Furthermore, this result suggests that a HFD accentuated abnormalities in calcium homeostasis in animals treated with PER. The observed Ca^{2+} overload could be related to the inhibition of sarco-/endoplasmic reticulum ATPase (SERCA2a), a known carrier of calcium from the cytosol to the SER for heart relaxation (Kronenbitter et al., 2018). Previously, a HFD or environmental pollutant exposure had been shown to disrupt endoplasmic reticulum calcium homeostasis by altering SERCA2a expression and activity (Patel et al., 2015; Wires et al., 2017).

Cardiac fibrosis has been associated with several cardiovascular failures (Moore-Morris et al., 2016). The present study showed that HFD and/or PER induced cardiac fibrosis, with animals receiving both HFD and PER exhibiting greater cardiac fibrosis. Fibrosis status resulted from the release of extracellular matrix (ECM) collagens, confirmed by

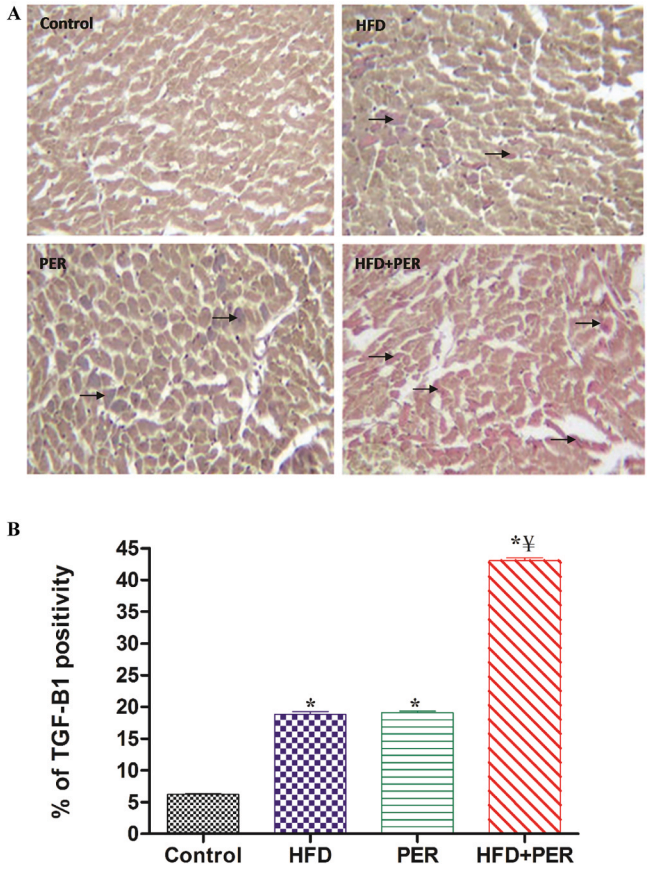

Fig. 6. Representative images for the immunochemical detection of TGF-β1 in cardiac tissue (A) and percentage quantification of TGF-β1 (B) in control and experimental treated rats (G × 200). Values are expressed as mean ± standard deviation for the 10 rats in each group. * $P<$ 0.05 significant differences compared to controls. ¥ $P<0.05$ significant differences compared to the high-fat diet or permethrin group.

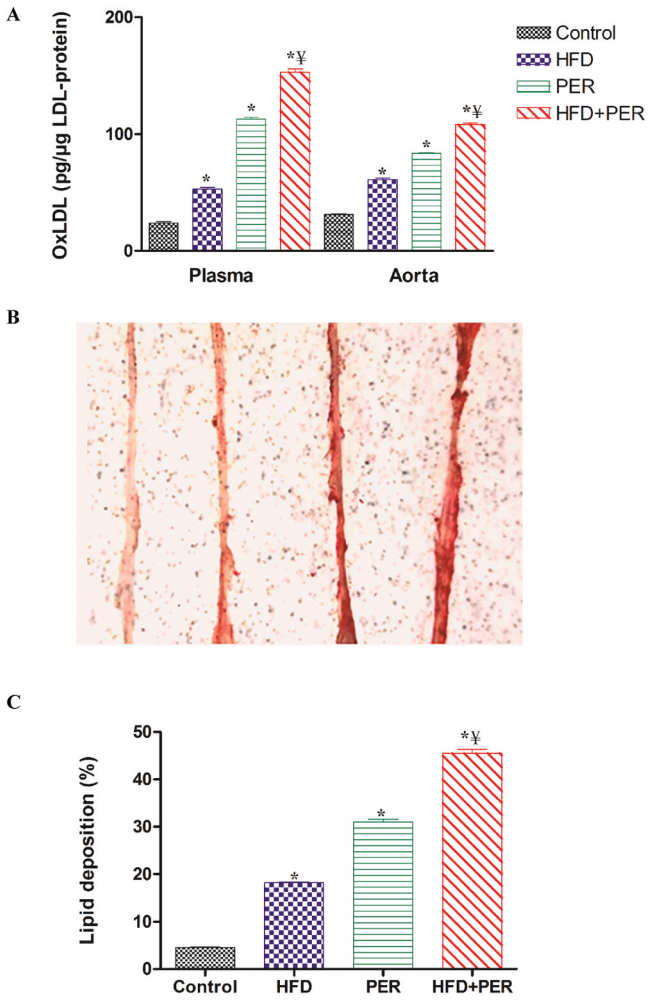

Fig. 7. Variations in plasma and aortic oxidized low-density lipoprotein (A) and photomicrographs of aortic tissue [Oil Red O staining (G × 200)] (B) from all experimental rats. The control group exhibited no lipid droplets. Arterial tissues of obese animals alone or those exposed to PER showed increased lipid deposits (red color) in the thickened intima. Values are expressed as mean ± standard deviation for the 10 rats in each group. *$P<$ 0.05 significant differences compared to controls. ¥ $P<0.05$ significant differences compared to the high-fat diet or permethrin group.

Masson's Trichrome staining of heart tissues. Similar results have been observed in Wistar rats fed a HFD or pyrethroid pesticides (Feriani et al., 2020d; Watanabe et al., 2018). The profibrotic effects of a HFD and/or PER could have resulted from the upregulation of collagen I and III mRNA in cardiac tissue, as reported previously by (Yu et al., 2020).

The potential mechanism by which a HFD and/or PER exposure contributed to cardiac fibrosis remains to be determined. Inflammation seems to be one possible explanation, as discussed previously (Li et al., 2017). Such findings had been confirmed in the present study, which showed elevated plasma and cardiac levels of TNF-α and IL-6, both proinflammatory molecules, after HFD and/or PER exposure a phenomenon that could activate synthesis of the ECM collagen gene (Kurose and Mangmool, 2016). The increased cytokine concentrations might be related to NF-κB activation via the free radical-mediated pathway (Feriani et al., 2020c). This hypothesis is supported by the current study where in cardiac NF-κB mRNA expression increased following HFD and/or PER treatment. Notably, rats exposed to HFD and PER had worse cardiac fibrosis perhaps because HFD potentiates the activation of inflammatory parameters, which in turn induce increased collagen I and III expression, thereby amplifying collagen deposition in the ECM. However, further studies are needed to validate this hypothesis. Furthermore, the association between TGF-β1/Smad signaling pathway activation and increased cardiac fibrosis has been widely accepted (Han et al., 2019). TGF-β1 has been considered an inductor of ECM synthesis and exerts its function through the Smad gene (Liu et al., 2019). Smad2 and Smad3 have been known as receptor-activated Smad proteins that can be phosphorylated by TGF-β1, with the resisting the complex being able to bind with Smad4 and initiate translocation into the nucleus to activate profibrotic genes (Ma et al., 2017). Accordingly, the current findings revealed that subchronic HFD and/or PER administration increased TGF-β1 expression in heart tissues. The upregulation of this gene could explain the observed fibrotic event. These findings have been corroborated by recent studies investigating the implication of TGF-β1/Smad signaling pathway in fibrotic events in either obese animals or those exposed to pyrethroid pesticide (Feriani et al., 2020c; Li et al., 2017). Moreover, this study has been the first to examine the possible fibrotic change in heart tissues among animals exposed to a HFD and pesticide.

The present study observed an apparent increase in plasma ox-LDL levels in HFD and/or PER-exposed rats. Generally, a hyperlipidemic diet or pyrethroid exposure has been associated with elevated circulating levels of ox-LDL (Feriani et al., 2020a, 2020d; Heriansyah et al., 2017). According to (Chatauret et al., 2014), elevated ox-LDL levels were significantly correlated with the activation of pro-fibrotic TGF-β1. Thus, these results suggest that ox-LDL was involved in the HFD- and/or PER-induced stimulation of the TGF-β1 pathway.

Our data also demonstrated that a HFD and/or PER administration was able to increase aortic levels of ox-LDL, a known lipid parameter

that contributes to the formation of fatty plaque in the arterial wall (Gao and Liu, 2017). Such findings were supported by Oil Red staining, which revealed the presence of several lipid droplets in the arterial tissues of rats. Previous reports corroborating this finding have demonstrated that HFD or pesticide exposure could induce elevated aortic lipid deposition in laboratory animals (Feriani et al., 2020a; Watanabe et al., 2018). Indeed, the presence of fat has been a common cause for the development of atherosclerosis, an event that contributed to cardiac ischemia (Libby et al., 2019). Interestingly, HFD aggravated lipid accumulation in arterial tissues of PER-treated rats. As discussed earlier, the metabolic phenotype associated with obesity may amplify pesticide-induced toxicity (Xiao et al., 2018). The observed effects could have resulted from the PER-induced upregulation of CD36 in obese animals. The scavenger receptor binds and internalizes ox-LDL in arterial tissues (Feriani et al., 2020d), favoring increased formation of foam cells and atheroma plaque. However, additional studies are necessary to verify this hypothesis.

5. Conclusion

Overall, the findings obtained herein suggest that subchronic post-weaning exposure to HFD and/or PER can alter cardiac integrity and induce heart fibrosis. This harmful effect could be mediated by oxidative stress, inflammation, apoptosis, and the TGF-β1/Smads signaling pathway, as well as the increase in ox-LDL associated with atherogenesis. The observed cardiac and arterial dysregulation had been exacerbated after consuming a HFD, supporting the increased internalization of PER, a lipophilic compound, in fat-rich tissues and consequent cardiotoxicity following its metabolism. Noticeably, the present findings are highly relevant for understanding the impact of lifelong exposure to food pollutants and their synergistic effects with an obesogenic diet, especially considering the worldwide context of high fat consumption and exposure to chemicals.

CRediT authorship contribution statement

Anouar Feriani: Conceptualization, Investigation, Methodology, Writing - original draft, Writing - review & editing. **Mariano Bizzarri:** Validation, Writing - review & editing. **Meriam Tir:** Investigation. **Nouf Aldawood:** Investigation. **Hussah Alobaid:** Methodology. **Mohamed Salah Allagui:** Supervision. **Waleed Dahmash:** Methodology. **Nizar Tlili:** Investigation, Methodology. **Kais Mnafgui:** Supervision. **Saleh Alwasel:** Project administration, Validation. **Abdel Halim Harrath:** Conceptualization, Project administration, Validation, Writing - original draft, Writing - review & editing.

Declaration of Competing Interest

The authors declare that they have no known competing financial interests or personal relationships that could have appeared to influence the work reported in this paper.

Acknowledgments

We are grateful to the facilities and the support provided by the director and technicians of the Anatomopathology Laboratory, Gafsa, Tunisia. The authors extend their appreciation to the Researchers Supporting Project number (RSP-2021/17) at King Saud University, Riyadh, Saudi Arabia.

References

Aebi, H., 1984. Catalase in vitro. Methods Enzymol. 105, 121–126.
Berg, Z.K., Rodriguez, B., Davis, J., Katz, A.R., Cooney, R.V., Masaki, K., 2019. Association between occupational exposure to pesticides and cardiovascular disease incidence: the Kuakini Honolulu heart program. J. Am. Heart Assoc. 8, 012569.
Buege, J.A., Aust, S.D., 1978. Microsomal lipid peroxidation. Methods Enzymol. 52, 302–310.
Chatauret, N., Favreau, F., Giraud, S., Thierry, A., Rossard, L., Le Pape, S., Lerman, L.O., Hauet, T., 2014. Diet-induced increase in plasma oxidized LDL promotes early fibrosis in a renal porcine auto-transplantation model. J. Transl. Med. 12, 76.
Chiu, Y.H., Sandoval-Insausti, H., Ley, S.H., Bhupathiraju, S.N., Hauser, R., Rimm, E.B., Manson, J.E., Sun, Q., Chavarro, J.E., 2019. Association between intake of fruits and vegetables by pesticide residue status and coronary heart disease risk. Environ. Int. 132, 105113.
Csige, I., Ujvarosy, D., Szabo, Z., Lorincz, I., Paragh, G., Harangi, M., Somodi, S., 2018. The impact of obesity on the cardiovascular system. J. Diabetes Res. 2018, 3407306.
Cui, G., Xin, Q., Tseng, H.H.L., Hoi, M.P., Wang, Y., Yang, B., Choi, I., Wang, Y., Yuan, R., Chen, K., Cong, W., Lee, S.M., 2018. A novel Ca(2+) current blocker promotes angiogenesis and cardiac healing after experimental myocardial infarction in mice. Pharm. Res. 134, 109–117.
Dziadek, K., Kopeć, A., Piątkowska, E., 2019. Intake of fruit and leaves of sweet cherry beneficially affects lipid metabolism, oxidative stress and inflammation in Wistar rats fed with high fat-cholesterol diet. J. Funct. Foods 57, 31–39.
El Khayat El Sabbouri, H., Gay-Queheillard, J., Joumaa, W.H., Delanaud, S., Guibourdenche, M., Darwiche, W., Djekkoun, N., Bach, V., Ramadan, W., 2020. Does the perigestational exposure to chlorpyrifos and/or high-fat diet affect respiratory parameters and diaphragmatic muscle contractility in young rats? Food Chem. Toxicol. 140, 111322.
Ellman, G.L., 1959. Tissue sulfhydryl groups. Arch. Biochem. Biophys. 82, 70–77.
Fedeli, D., Montani, M., Bordoni, L., Galeazzi, R., Nasuti, C., Correia-Sá, L., Domingues, V.F., Jayant, M., Brahmachari, V., Massaccesi, L., Laudadio, E., Gabbianelli, R., 2017. In vivo and in silico studies to identify mechanisms associated with Nurr1 modulation following early life exposure to permethrin in rats. Neuroscience 340, 411–423.
Feriani, A., Hachani, R., Tir, M., Ghazouani, L., Mufti, A., Borgi, M.A., Allagui, M.S., 2020a. Bifenthrin exerts proatherogenic effects via arterial accumulation of native and oxidized LDL in rats: the beneficial role of vitamin E and selenium. Environ. Sci. Pollut. Res. Int. 27, 5651–5660.
Feriani, A., Tir, M., Gómez-Caravaca, A.M., Contreras, M.M., Talhaoui, N., Taamalli, A., Segura-Carretero, A., Ghazouani, L., Mufti, A., Tlili, N., Allagui, M.S., 2020b. HPLC-DAD-ESI-QTOF-MS/MS profiling of Zygophyllum album roots extract and assessment of its cardioprotective effect against deltamethrin-induced myocardial injuries in rat, by suppression of oxidative stress-related inflammation and apoptosis via NF-κB signaling pathway. J. Ethnopharmacol. 247, 112266.
Feriani, A., Tir, M., Gomez-Caravaca, A.M., Del Mar Contreras, M., Taamalli, A., Segura-Carretero, A., Ghazouani, L., Mufti, A., Tlili, N., El Feki, A., et al., 2020c. Zygophyllum album leaves extract prevented hepatic fibrosis in rats, by reducing liver injury and suppressing oxidative stress, inflammation, apoptosis and the TGF-beta1/Smads signaling pathways. Exploring of bioactive compounds using HPLC-DAD-ESI-QTOF-MS/MS. Inflammopharmacology.
Feriani, A., Tir, M., Hachani, R., Allagui, M.S., Tlili, N., Nahdi, S., Alwasel, S., Harrath, A. H., 2021. Permethrin induced arterial retention of native and oxidized LDL in rats by promoting inflammation, oxidative stress and affecting LDL receptors, and collagen genes. Ecotoxicol. Environ. Saf. 207, 111269.
Feriani, A., Tir, M., Hachani, R., Gómez-Caravaca, A.M., Contreras, M.M., Taamalli, A., Talhaoui, N., Segura-Carretero, A., Ghazouani, L., Mufti, A., Tlili, N., El Feki, A., Harrath, A.H., Allagui, M.S., 2020d. Zygophyllum album saponins prevent atherogenic effect induced by deltamethrin via attenuating arterial accumulation of native and oxidized LDL in rats. Ecotoxicol. Environ. Saf. 193, 110318.
Flohe, L., Gunzler, W.A., 1984. Assays of glutathione peroxidase. Methods Enzymol. 105, 114–121.
Gao, S., Liu, J., 2017. Association between circulating oxidized low-density lipoprotein and atherosclerotic cardiovascular disease. Chronic Dis. Transl. Med. 3, 89–94.
Gargouri, B., Yousif, N.M., Attaai, A., Bouchard, M., Chtourou, Y., Fiebich, B.L., Fetoui, H., 2018. Pyrethroid bifenthrin induces oxidative stress, neuroinflammation, and neuronal damage, associated with cognitive and memory impairment in murine hippocampus. Neurochem. Int. 120, 121–133.
Georgiadis, N., Tsarouhas, K., Tsitsimpikou, C., Vardavas, A., Rezaee, R., Germanakis, I., Tsatsakis, A., Stagos, D., Kouretas, D., 2018. Pesticides and cardiotoxicity. Where do we stand? Toxicol. Appl. Pharm. 353, 1–14.
Hamzeh, N., Ghadimi, F., Farzaneh, R., Hosseini, S.K., 2017. Obesity, heart failure, and obesity paradox. J. Tehran Heart Cent. 12, 1–5.
Han, X., Li, M., Zhao, Z., Zhang, Y., Zhang, J., Zhang, X., Zhang, Y., Guan, S., Chu, L., 2019. Mechanisms underlying the cardio-protection of total ginsenosides against myocardial ischemia in rats in vivo and in vitro: possible involvement of L-type Ca(2+) channels, contractility and Ca(2+) homeostasis. J. Pharm. Sci. 139, 240–248.
Heriansyah, T., Adam, A., Wihastuti, T., Rohman, M., 2017. Elaborate evaluation of serum and tissue oxidized LDL level with darapladib therapy: a feasible diagnostic marker for early atherogenesis. Asian Pac. J. Trop. Biomed. 7, 134–138.
Hladik, M.L., Kuivila, K.M., 2009. Assessing the occurrence and distribution of pyrethroids in water and suspended sediments. J. Agric. Food Chem. 57, 9079–9085.
Howell 3rd, G.E., Kondakala, S., Holdridge, J., Lee, J.H., Ross, M.K., 2018. Inhibition of cholinergic and non-cholinergic targets following subacute exposure to chlorpyrifos in normal and high fat fed male C57BL/6J mice. Food Chem. Toxicol. 118, 821–829.
Howell 3rd, G.E., Mulligan, C., Meek, E., Chambers, J.E., 2015. Effect of chronic p,p′-dichlorodiphenyldichloroethylene (DDE) exposure on high fat diet-induced alterations in glucose and lipid metabolism in male C57BL/6H mice. Toxicology 328, 112–122.
IRIS, 1998. Integrated Risk Information System. US Environmental Protection Agency, Washington DC (version CD-ROM), MICROMEDEX, Inc., Englewood, Colorado.

Jellali, R., Zeller, P., Gilard, F., Legendre, A., Fleury, M.J., Jacques, S., Tcherkez, G., Leclerc, E., 2018. Effects of DDT and permethrin on rat hepatocytes cultivated in microfluidic biochips: metabolomics and gene expression study. Environ. Toxicol. Pharm. 59, 1–12.

Karmaus, A.L., Filer, D.L., Martin, M.T., Houck, K.A., 2016. Evaluation of food-relevant chemicals in the ToxCast high-throughput screening program. Food Chem. Toxicol. 92, 188–196.

Kim, M.J., Lee, K.J., Hwang, J.Y., Lee, H.S., Chio, S.H., Lim, S., Jang, H.C., Park, Y.J., 2013. Loss of small heterodimer partner protects against atherosclerosis in apolipoprotein E-deficient mice. Endocr. J. 60, 1171–1177.

Kim, T.W., Kim, Y.J., Seo, C.S., Kim, H.T., Park, S.R., Lee, M.Y., Jung, J.Y., 2016. Elsholtzia ciliata (Thunb.) Hylander attenuates renal inflammation and interstitial fibrosis via regulation of TGF-ss and Smad3 expression on unilateral ureteral obstruction rat model. Phytomedicine 23, 331–339.

Kondakala, S., Lee, J.H., Ross, M.K., Howell 3rd, G.E., 2017. Effects of acute exposure to chlorpyrifos on cholinergic and non-cholinergic targets in normal and high-fat fed male C57BL/6J mice. Toxicol. Appl. Pharm. 337, 67–75.

Kronenbitter, A., Funk, F., Hackert, K., Gorreßen, S., Glaser, D., Boknik, P., Poschmann, G., Stühler, K., Isić, M., Krüger, M., Schmitt, J.P., 2018. Impaired Ca(2+) cycling of nonischemic myocytes contributes to sarcomere dysfunction early after myocardial infarction. J. Mol. Cell. Cardiol. 119, 28–39.

Kumar, A., Sasmal, D., Sharma, N., 2015. An insight into deltamethrin induced apoptotic calcium, p53 and oxidative stress signalling pathways. Toxicol. Environ. Health Sci. 7, 25–34.

Kurose, H., Mangmool, S., 2016. Myofibroblasts and inflammatory cells as players of cardiac fibrosis. Arch. Pharm. Res. 39, 1100–1113.

Levine, R.L., Garland, D., Oliver, C.N., Amici, A., Climent, I., Lenz, A.G., Ahn, B.W., Shaltiel, S., Stadtman, E.R., 1990. Determination of carbonyl content in oxidatively modified proteins. Methods Enzymol. 186, 464–478.

Li, S.J., Liu, C.H., Chu, H.P., Mersmann, H.J., Ding, S.T., Chu, C.H., Wang, C.Y., Chen, C. Y., 2017. The high-fat diet induces myocardial fibrosis in the metabolically healthy obese minipigs-the role of ER stress and oxidative stress. Clin. Nutr. 36, 760–767.

Li, W., Morgan, M.K., Graham, S.E., Starr, J.M., 2016. Measurement of pyrethroids and their environmental degradation products in fresh fruits and vegetables using a modification of the quick easy cheap effective rugged safe (QuEChERS) method. Talanta 151, 42–50.

Libby, P., Buring, J.E., Badimon, L., Hansson, G.K., Deanfield, J., Bittencourt, M.S., Tokgozoglu, L., Lewis, E.F., 2019. Atherosclerosis. Nat. Rev. Dis. Prim. 5, 56.

Liu, B., Rong, Y., Sun, D., Li, W., Chen, H., Cao, B., Wang, T., 2019. Costunolide inhibits pulmonary fibrosis via regulating NF-kB and TGF-beta1/Smad2/Nrf2-NOX4 signaling pathways. Biochem. Biophys. Res. Commun. 510, 329–333.

Liu, C., Yang, Q., Fang, G., Li, B.S., Wu, D.B., Guo, W.J., Hong, S.S., Hong, L., 2016. Collagen metabolic disorder induced by oxidative stress in human uterosacral ligamentderived fibroblasts: a possible pathophysiological mechanism in pelvic organ prolapse. Mol. Med. Rep. 13, 2999–3008.

Ma, T., Cai, X., Wang, Z., Huang, L., Wang, C., Jiang, S., Hua, Y., Liu, Q., 2017. miR-200c accelerates hepatic stellate cell-induced liver fibrosis via targeting the FOG2/PI3K pathway. Biomed. Res. Int. 2017, 2670658.

Marklund, S., Marklund, G., 1974. Involvement of the superoxide anion radical in the autoxidation of pyrogallol and a convenient assay for superoxide dismutase. Eur. J. Biochem. 47, 469–474.

Moore-Morris, T., Cattaneo, P., Puceat, M., Evans, S.M., 2016. Origins of cardiac fibroblasts. J. Mol. Cell. Cardiol. 91, 1–5.

Nan, Y., Yi, S.J., Zhu, H.L., Xiong, Y.W., Shi, X.T., Cao, X.L., Zhang, C., Gao, L., Zhao, L. L., Zhang, J., Xu, D.X., Wang, H., 2020. Paternal cadmium exposure increases the susceptibility to diet-induced testicular injury and spermatogenic disorders in mouse offspring. Chemosphere 246, 125776.

Patel, B.B., Raad, M., Sebag, I.A., Chalifour, L.E., 2015. Sex-specific cardiovascular responses to control or high fat diet feeding in C57bl/6 mice chronically exposed to bisphenol A. Toxicol. Rep. 2, 1310–1318.

Prasad, E.M., Mopuri, R., Islam, M.S., Kodidhela, L.D., 2017. Cardioprotective effect of Vitex negundo on isoproterenol-induced myocardial necrosis in wistar rats: a dual approach study. Biomed. Pharm. 85, 601–610.

Ruan, X.H., Ma, T., Fan, Y., 2019. Ablation of TMEM126B protects against heart injury via improving mitochondrial function in high fat diet (HFD)-induced mice. Biochem. Biophys. Res. Commun. 515, 636–643.

Saillenfait, A.M., Sabate, J.P., Denis, F., Antoine, G., Robert, A., Eljarrat, E., 2018. The pyrethroid insecticides permethrin and esfenvalerate do not disrupt testicular steroidogenesis in the rat fetus. Toxicology 410, 116–124.

Salmas, R.E., Gulhan, M.F., Durdagi, S., Sahna, E., Abdullah, H.I., Selamoglu, Z., 2017. Effects of propolis, caffeic acid phenethyl ester, and pollen on renal injury in hypertensive rat: an experimental and theoretical approach. Cell Biochem. Funct. 35, 304–314.

Sousa, T., Reina-Couto, M., Gomes, P., 2019. Role of oxidative stress in the pathophysiology of arterial hypertension and heart failure. Oxid. Stress Heart Dis. 509–537.

Talas, Z.S., Ozdemir, I., Ciftci, O., Cakir, O., Gulhan, M.F., Pasaoglu, O.M., 2014. Role of propolis on biochemical parameters in kidney and heart tissues against L-NAME induced oxidative injury in rats. Clin. Exp. Hypertens. 36, 492–496.

van der Pol, A., van Gilst, W.H., Voors, A.A., van der Meer, P., 2019. Treating oxidative stress in heart failure: past, present and future. Eur. J. Heart Fail. 21, 425–435.

Vijayakumar, R., Nachiappan, V., 2017. Cassia auriculata flower extract attenuates hyperlipidemia in male Wistar rats by regulating the hepatic cholesterol metabolism. Biomed. Pharm. 95, 394–401.

Vonderheide, A.P., Boyd, B., Ryberg, A., Yilmaz, E., Hieber, T.E., Kauffman, P.E., Garris, S.T., Morgan, J.N., 2009. Analysis of permethrin isomers in composite diet samples by molecularly imprinted solid-phase extraction and isotope dilution gas chromatography-ion trap mass spectrometry. J. Chromatogr. A 1216, 4633–4640.

Wang, D., Wang, X., Zhang, P., Wang, Y., Zhang, R., Yan, J., Zhou, Z., Zhu, W., 2017. The fate of technical-grade chlordane in mice fed a high-fat diet and its roles as a candidate obesogen. Environ. Pollut. 222, 532–542.

Watanabe, S., Kumazaki, S., Kusunoki, K., Inoue, T., Maeda, Y., Usui, S., Shinohata, R., Ohtsuki, T., Hirohata, S., Kusachi, S., Kitamori, K., Mori, M., Yamori, Y., Oka, H., 2018. A high-fat and high-cholesterol diet induces cardiac fibrosis, vascular endothelial, and left ventricular diastolic dysfunction in SHRSP5/Dmcr Rats. J. Atheroscler. Thromb. 25, 439–453.

WHO, 1996. WHO Recomm. Classif. Pestic. Hazard Guidel. Classif., 1996-1997.

Wires, E.S., Trychta, K.A., Back, S., Sulima, A., Rice, K.C., Harvey, B.K., 2017. High fat diet disrupts endoplasmic reticulum calcium homeostasis in the rat liver. J. Hepatol. 67, 1009–1017.

Xiao, X., Kim, Y., Kim, D., Yoon, K.S., Clark, J.M., Park, Y., 2017. Permethrin alters glucose metabolism in conjunction with high fat diet by potentiating insulin resistance and decreases voluntary activities in female C57BL/6J mice. Food Chem. Toxicol. 108, 161–170.

Xiao, X., Sun, Q., Kim, Y., Yang, S.H., Qi, W., Kim, D., Yoon, K.S., Clark, J.M., Park, Y., 2018. Exposure to permethrin promotes high fat diet-induced weight gain and insulin resistance in male C57BL/6J mice. Food Chem. Toxicol. 111, 405–416.

Yu, B., Yu, M., Zhang, H., Xie, D., Nie, W., Shi, K., 2020. Suppression of miR-143-3p contributes to the anti-fibrosis effect of atorvastatin on myocardial tissues via the modulation of Smad2 activity. Exp. Mol. Pathol. 112, 104346.

Zhang, L., Wei, J., Duan, J., Guo, C., Zhang, J., Ren, L., Liu, J., Li, Y., Sun, Z., Zhou, X., 2020. Silica nanoparticles exacerbates reproductive toxicity development in high-fat diet-treated Wistar rats. J. Hazard. Mater. 384, 121361.